– Supplementary Online Material –

Population coding for visual and auditory quantity in human numerotopic maps

Joram Soch[1,4], Anne-Sophie Kieslinger[1,4], Robert Trampel[2], Andreas Nieder[3] and Michael A. Skeide[1] ✉

[1] Research Group Learning in Early Childhood,
Max Planck Institute for Human Cognitive and Brain Sciences,
Stephanstraße 1A, 04103 Leipzig, Germany

[2] Department of Neurophysics,
Max Planck Institute for Human Cognitive and Brain Sciences,
Stephanstraße 1A, 04103 Leipzig, Germany

[3] Animal Physiology Unit, Institute of Neurobiology,
Eberhard-Karls-Universität Tübingen,
Auf der Morgenstelle 28, 72076 Tübingen, Germany

[4] These authors contributed equally: Joram Soch, Anne-Sophie Kieslinger.

✉ e-mail: skeide@cbs.mpg.de

Correspondence should be addressed to Michael A. Skeide

Supplementary Tables

subject ID	gender	age	visual hit rate	auditory hit rate
001	F	27,5	99,42	78,75
002	M	26	99,42	80,42
003	M	22	99,42	79,58
004	F	30,5	100,00	78,75
005	F	24,5	99,13	83,33
006	M	20	99,42	77,08
007	F	20	99,71	80,00
008	M	27	100,00	83,33
009	F	22	99,71	79,58
010	M	22	100,00	81,67
011	F	34	100,00	81,67
012	M	33,5	100,00	80,42

Table S1: Participant details. Pseudonymous subject ID, gender (F = female, M = male) and age in years (broken number when age changed across scanning sessions) as well as catch trial hit rates for the two modalities in percent (averaged across runs).

Figure	tuning parameters	native coordinates	standard coordinates	anatomical location (AAL regions)
2a/b	mu = 1.80, fwhm = 3.31	[-18, -27, 54]	[-29, -52, 46]	Parietal_Inf_L (NPC1)
2c/d	mu = 4.05, fwhm = 13.7	[-50, -45, 6]	[-43, -75, -3]	Occipital_Inf_L (NTO)
2e/f	mu = 1.85, fwhm = 26.0	[-42, -9, 22]	[-50, -33, 10]	Temporal_Sup_L (NaT)
2g/h	mu = 3.30, fwhm = 34.5	[-46, -7, 20]	[-54, -29, 8]	Temporal_Sup_L (NaT)

Table S2: Anatomical locations. Automated anatomical labeling (AAL) regions for vertices reported in Figure 2. All vertices are in the left hemisphere. Auditory locations in “Temporal_Sup_L” are close to “Temporal_Mid_L”.

Supplementary Figures

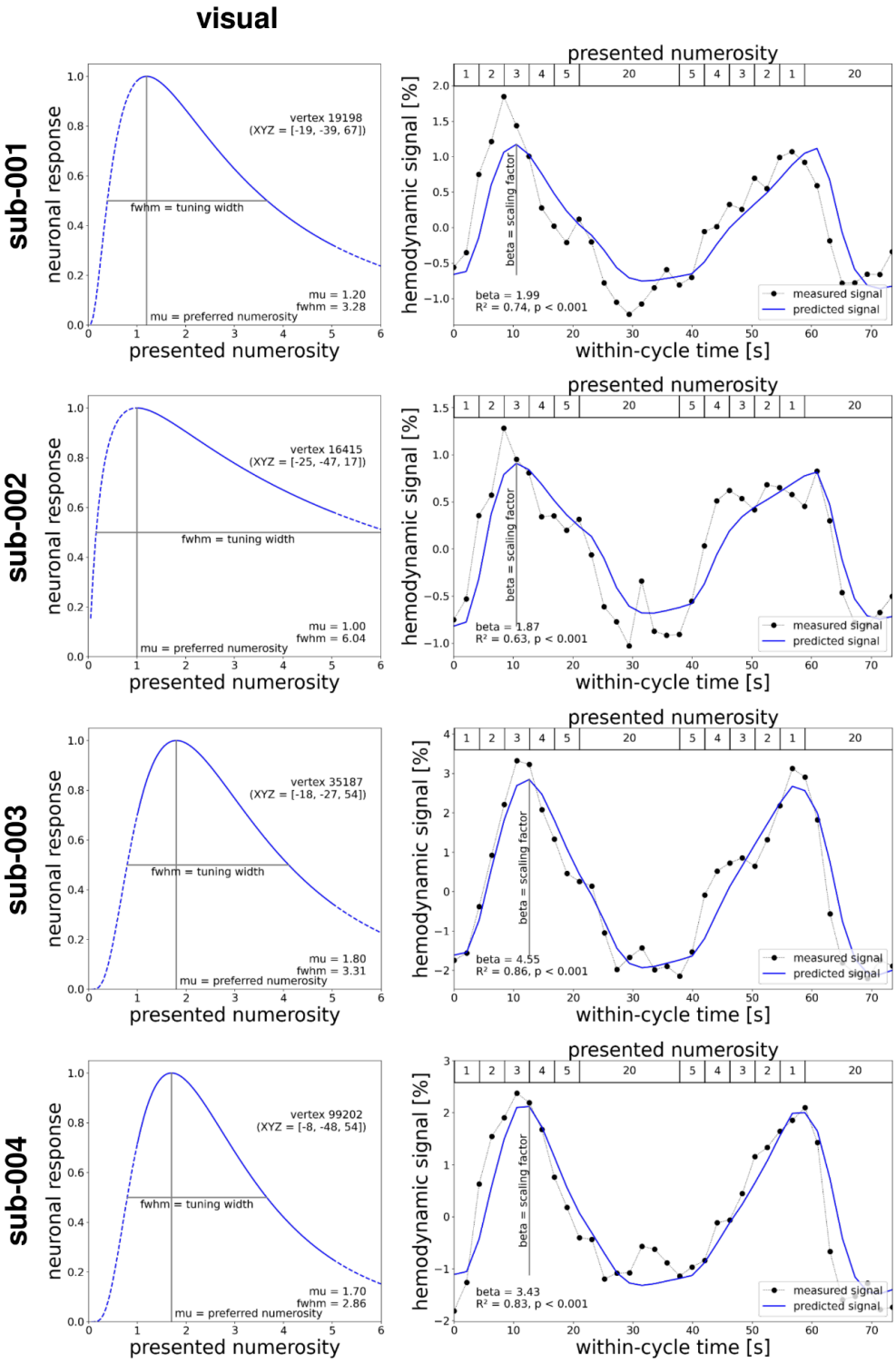

Figure S1: Neural tuning and hemodynamic responses to visual numerosity (page 1 of 3). Neural response functions (left) and hemodynamic responses measured using fMRI during visual numerosity presentation (right) were extracted from the vertex with the highest R^2.

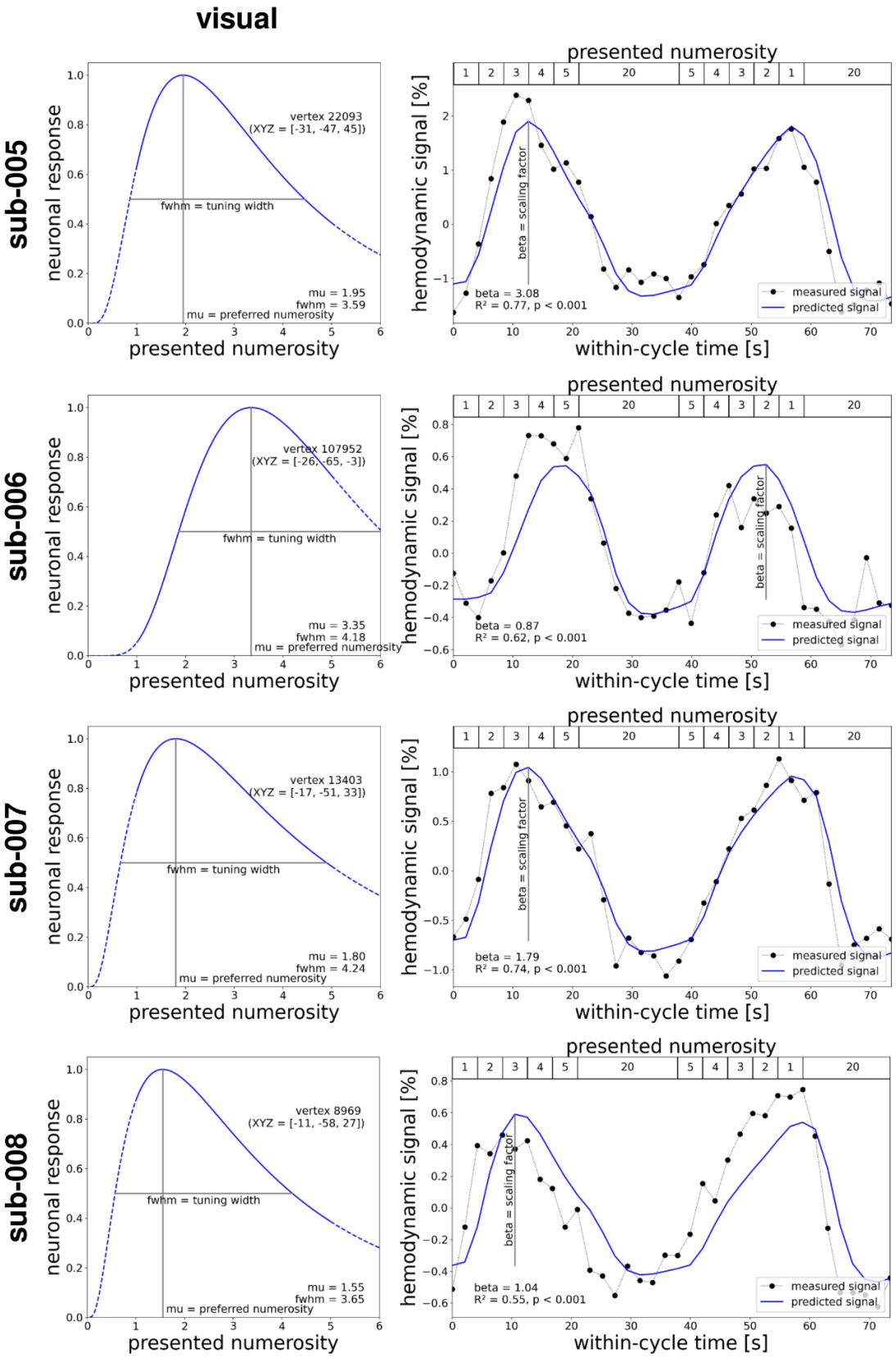

Figure S1: Neural tuning and hemodynamic responses to visual numerosity (page 2 of 3).

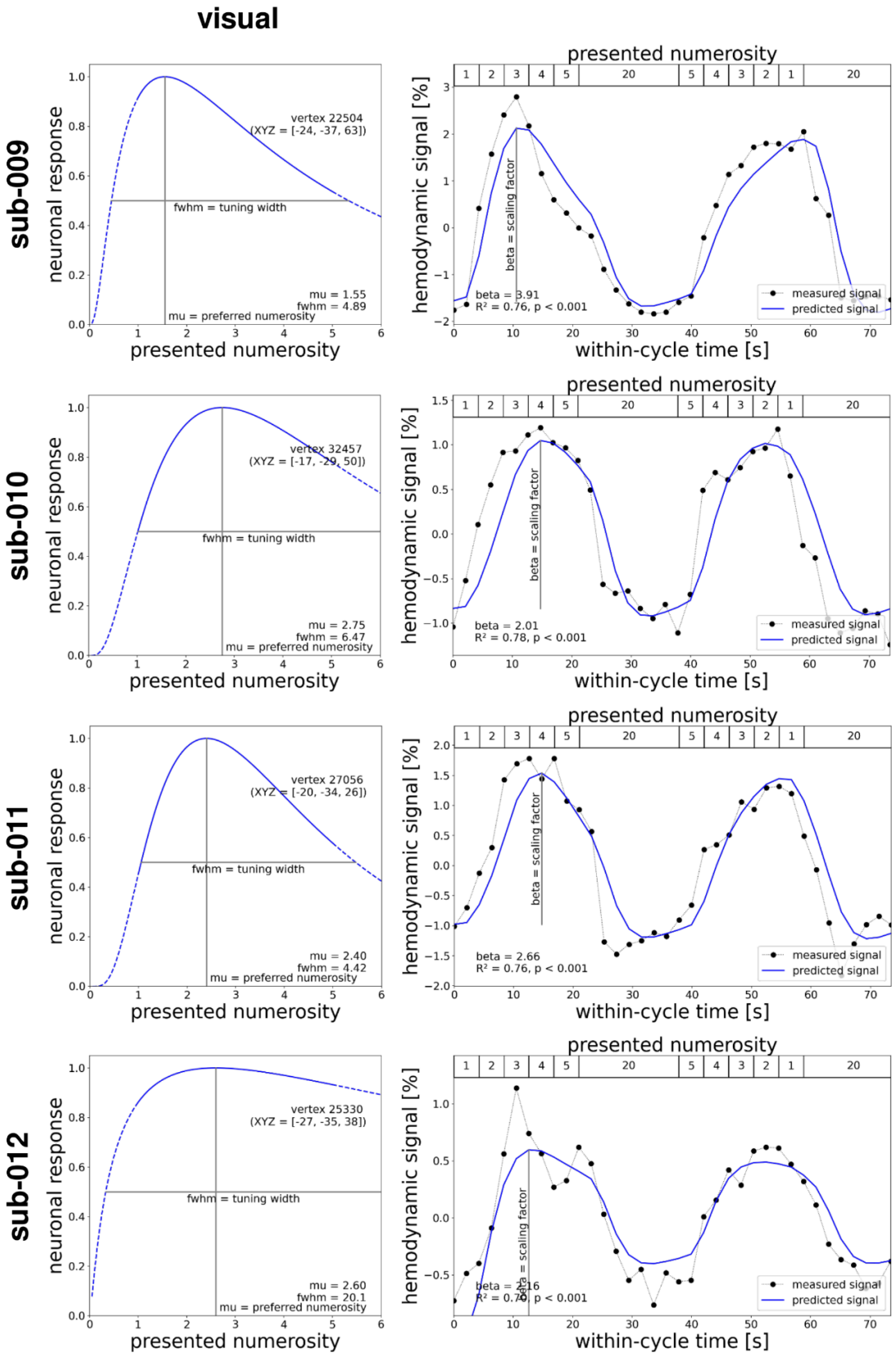

Figure S1: Neural tuning and hemodynamic responses to visual numerosity (page 3 of 3).

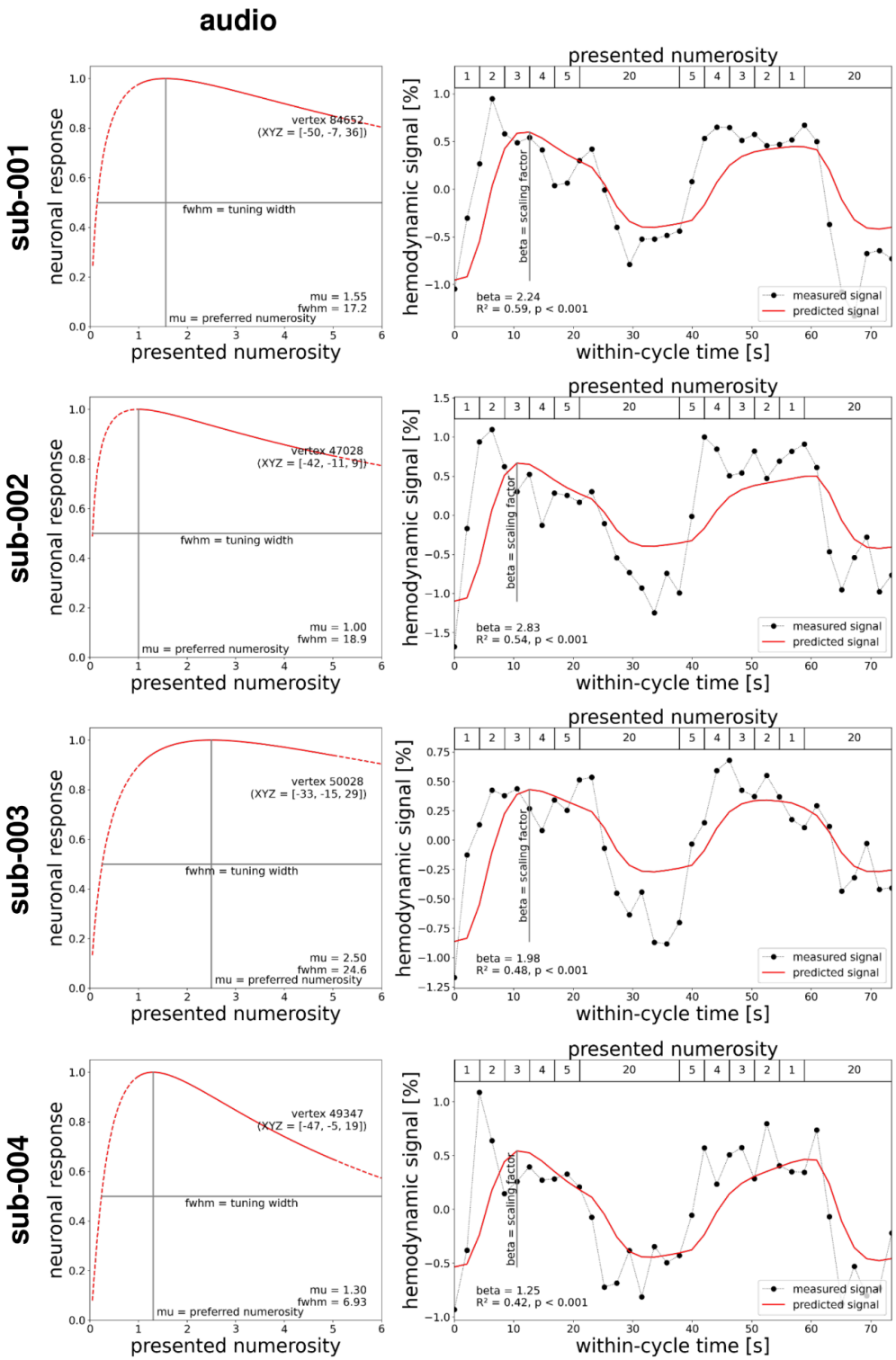

Figure S2: Neural tuning and hemodynamic responses to auditory numerosity (page 1 of 3). Neural response functions (left) and hemodynamic responses measured using fMRI during auditory numerosity presentation (right) were extracted from the vertex with the highest R^2

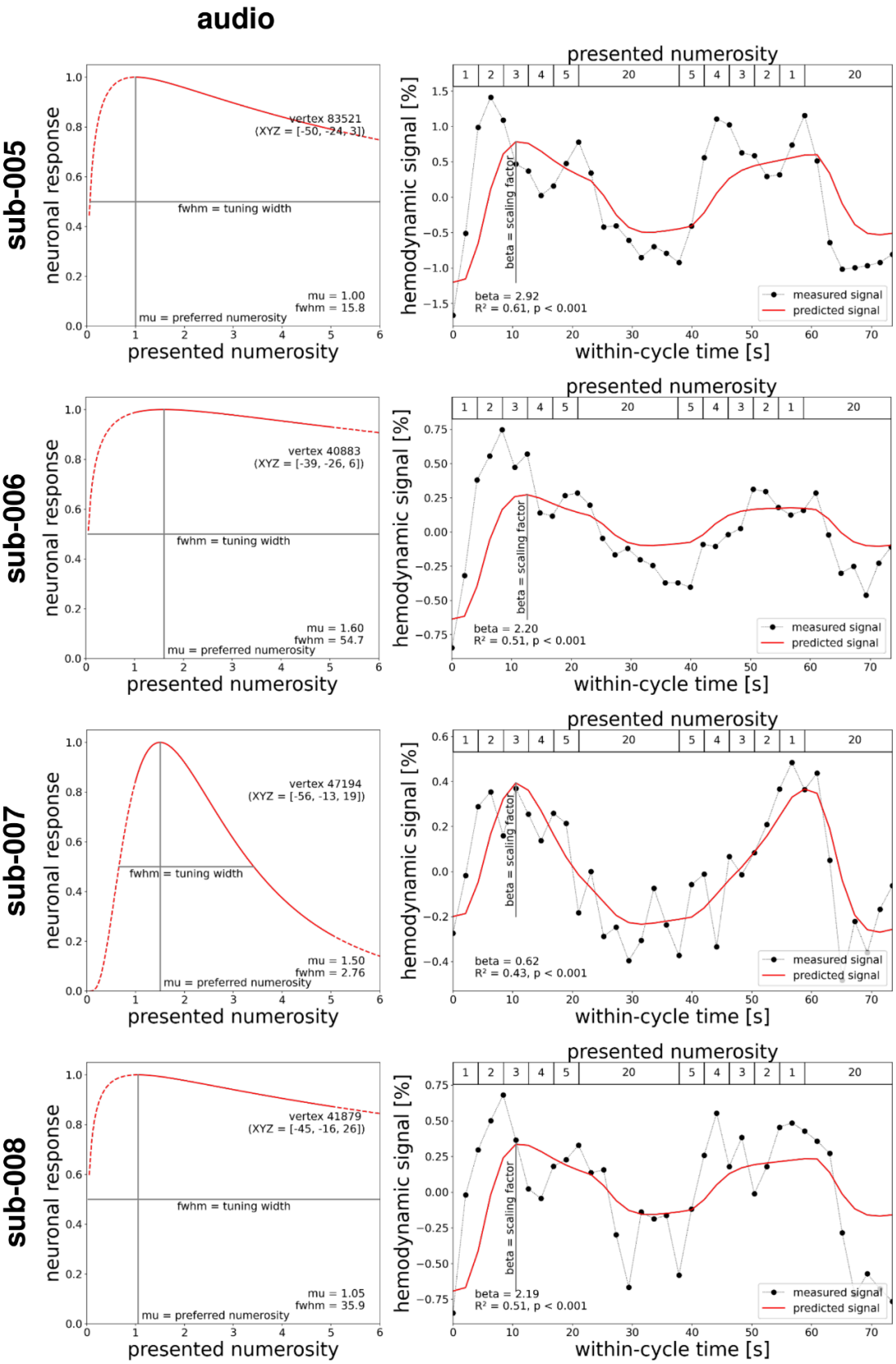

Figure S2: Neural tuning and hemodynamic responses to auditory numerosity (page 2 of 3).

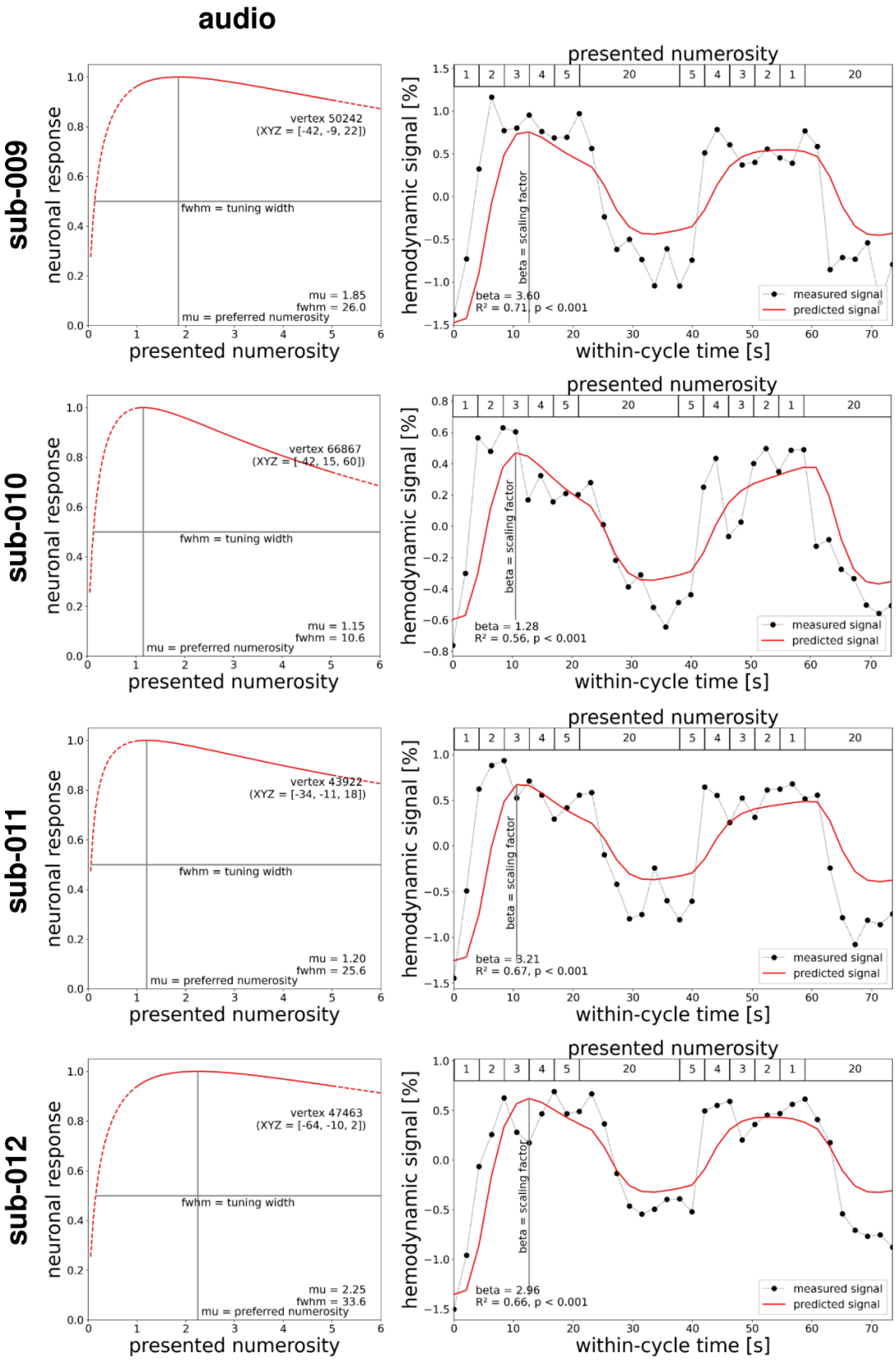

Figure S2: Neural tuning and hemodynamic responses to auditory numerosity (page 3 of 3).

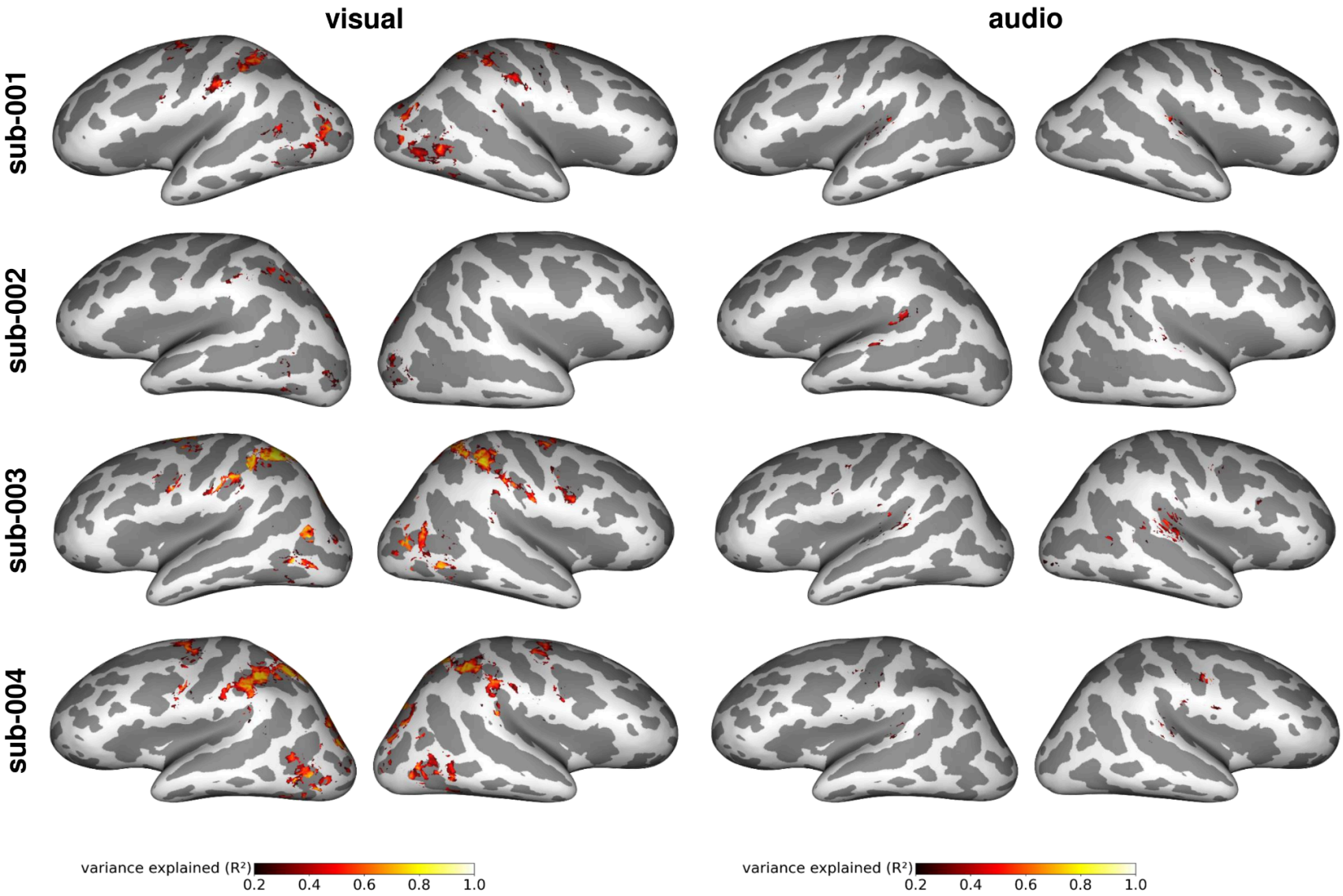

Figure S3: Variance explained by the neural tuning model (page 1 of 3). Inflated surface maps show R^2 of vertices in each subject's native space in which the neural tuning model explains at least 20% of the variance during visual and auditory numerosity perception.

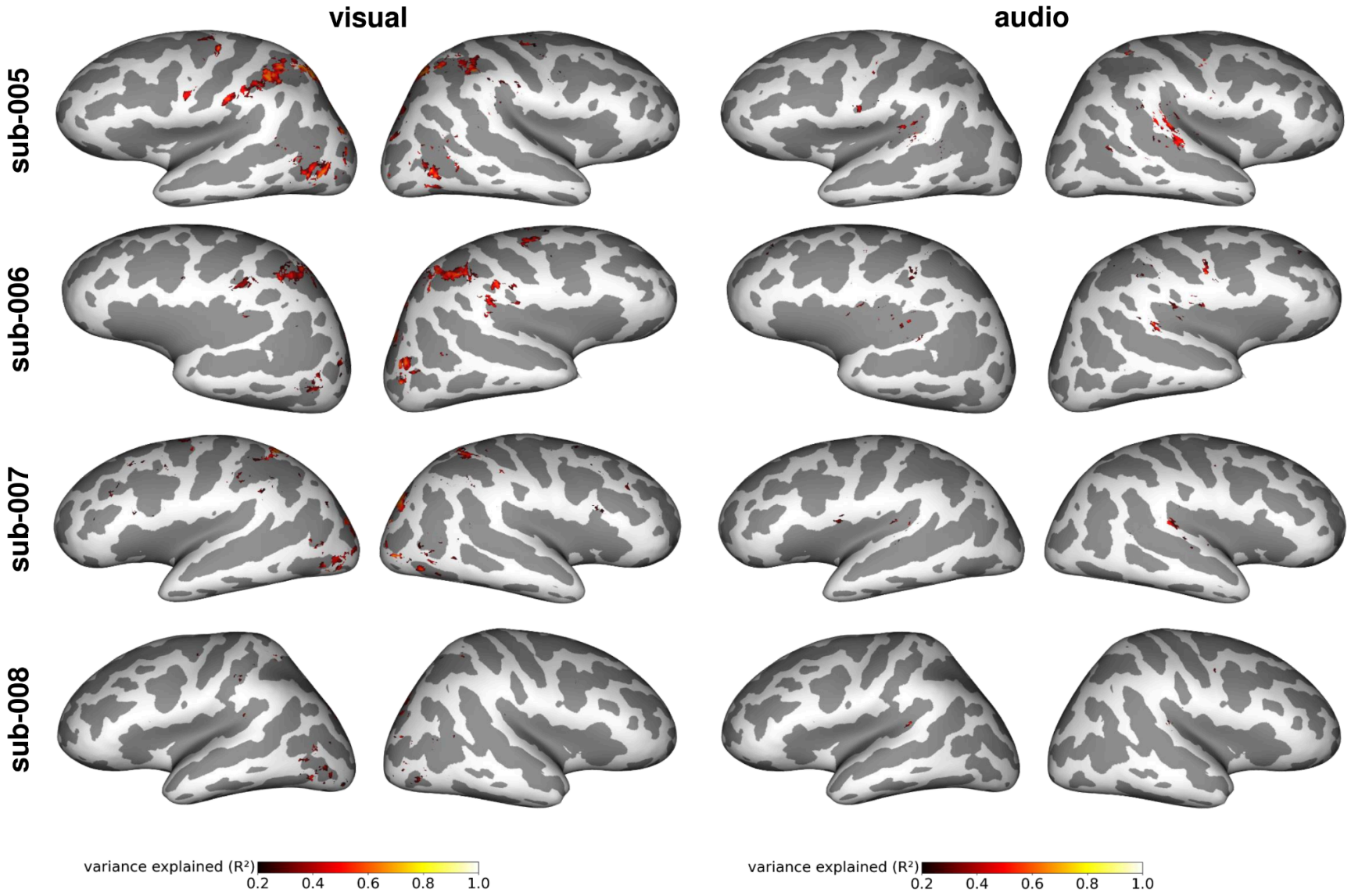

Figure S3: Variance explained by the neural tuning model (page 2 of 3).

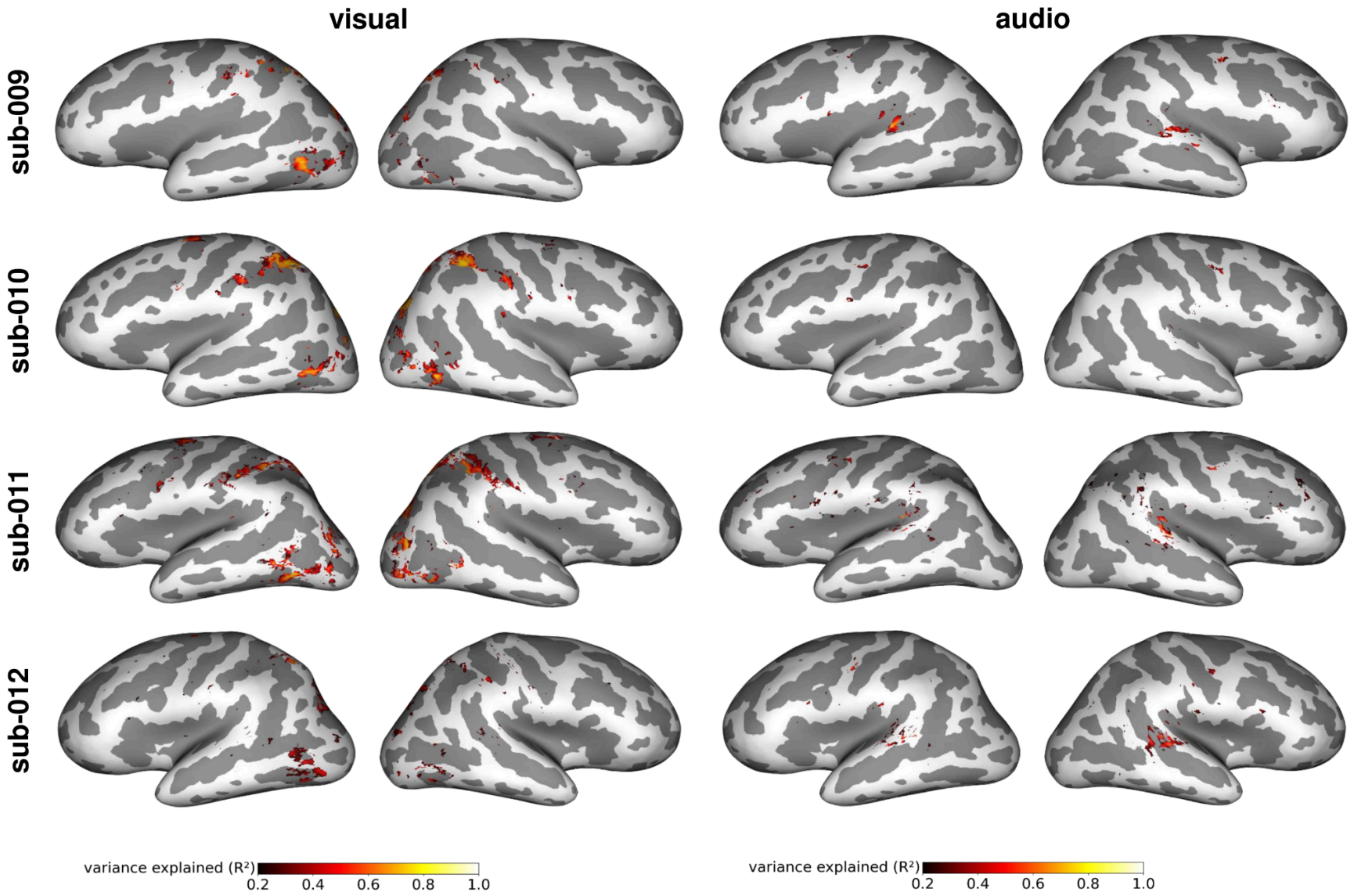

Figure S3: Variance explained by the neural tuning model (page 3 of 3).

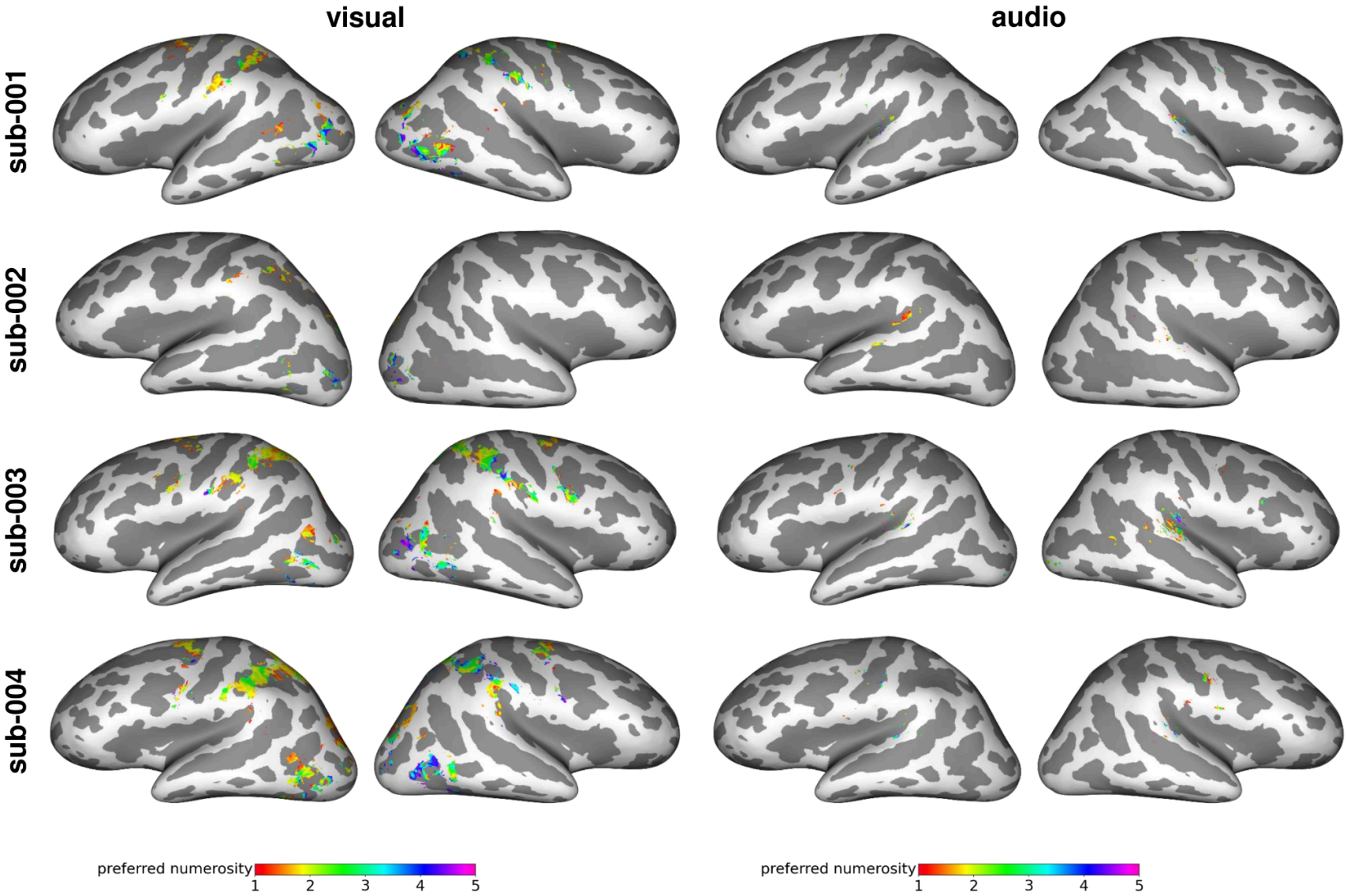

Figure S4: Preferred numerosity maps (page 1 of 3). Inflated surface maps show preferred numerosity of vertices in each subject's native space in which the neural tuning model explains at least 20% of the variance during visual and auditory numerosity perception.

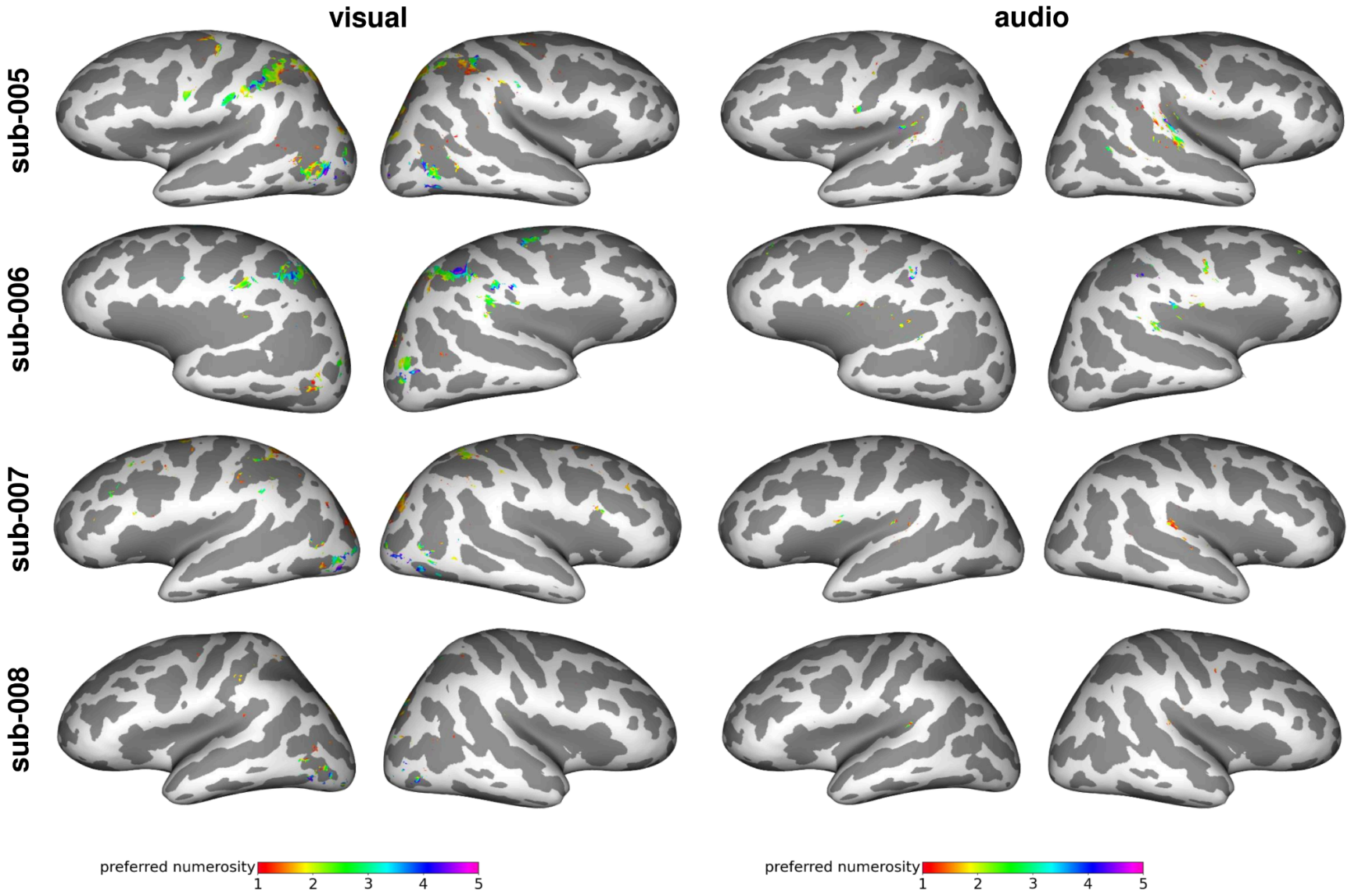

Figure S4: Preferred numerosity maps (page 2 of 3).

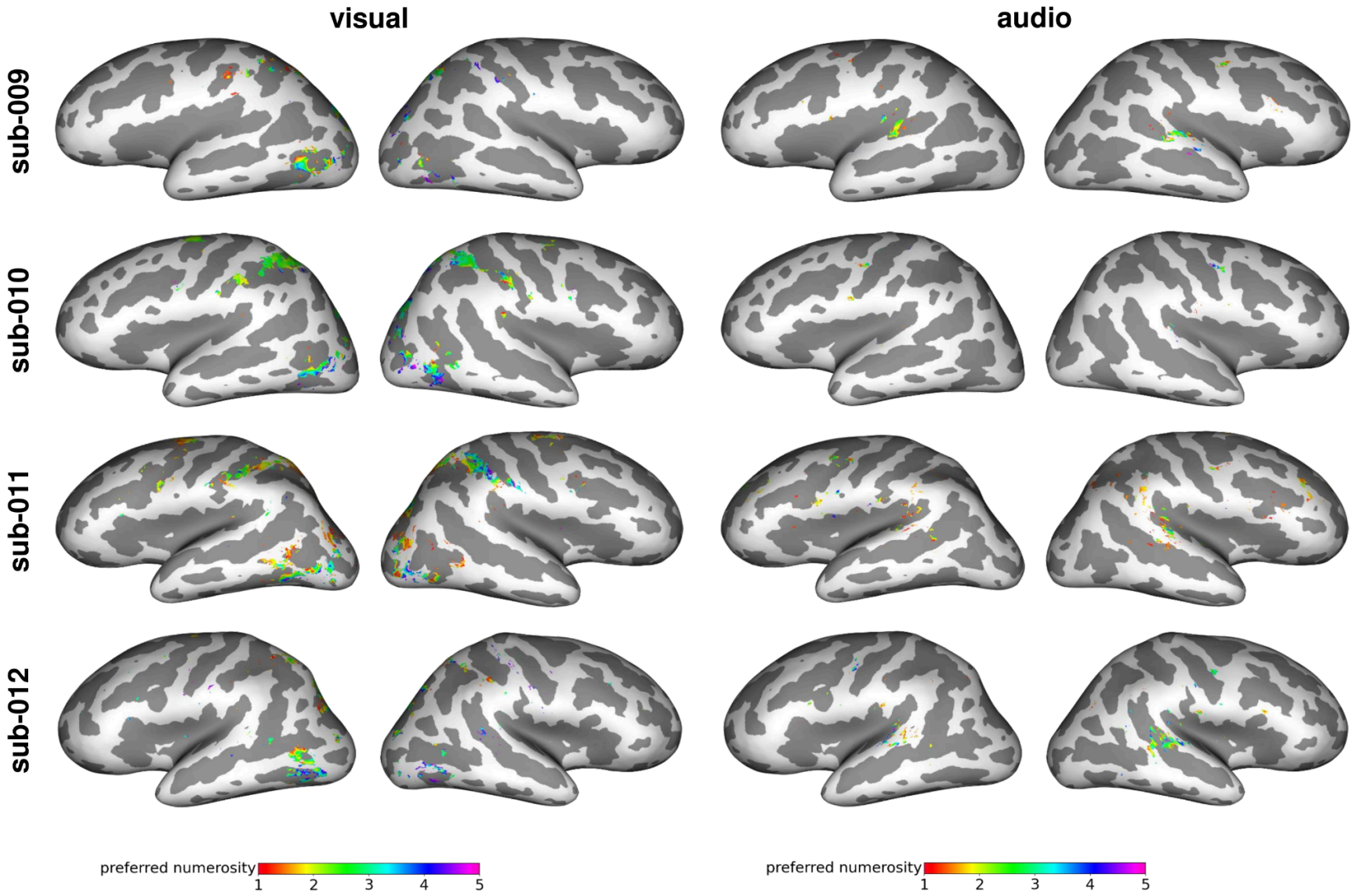

Figure S4: Preferred numerosity maps (page 3 of 3).

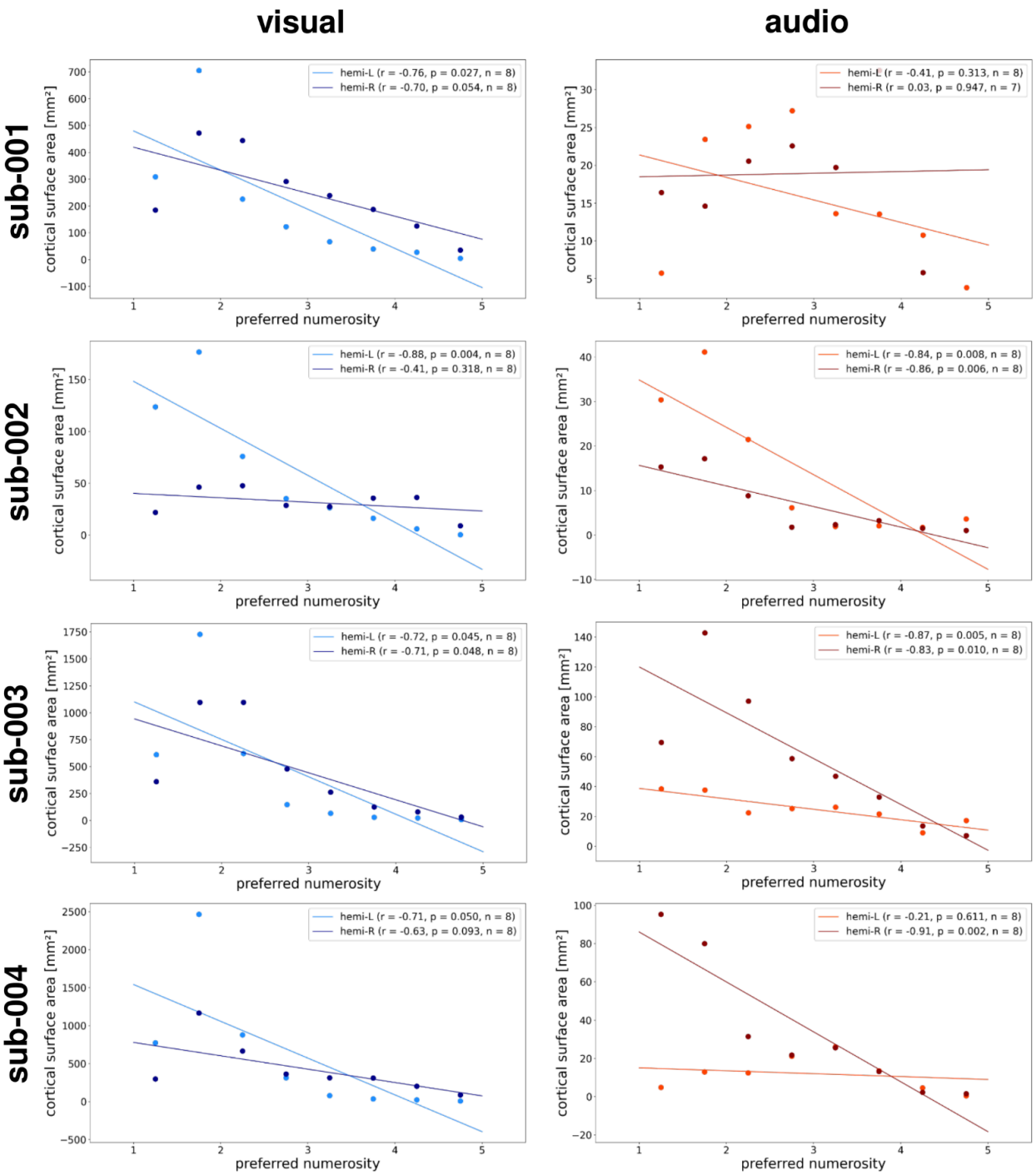

Figure S5: Linear associations between preferred numerosity and surface area (page 1 of 3). Cortical surface area decreases as a function of preferred numerosity in each subject perceiving either visual (left) or auditory (right) numerosity.

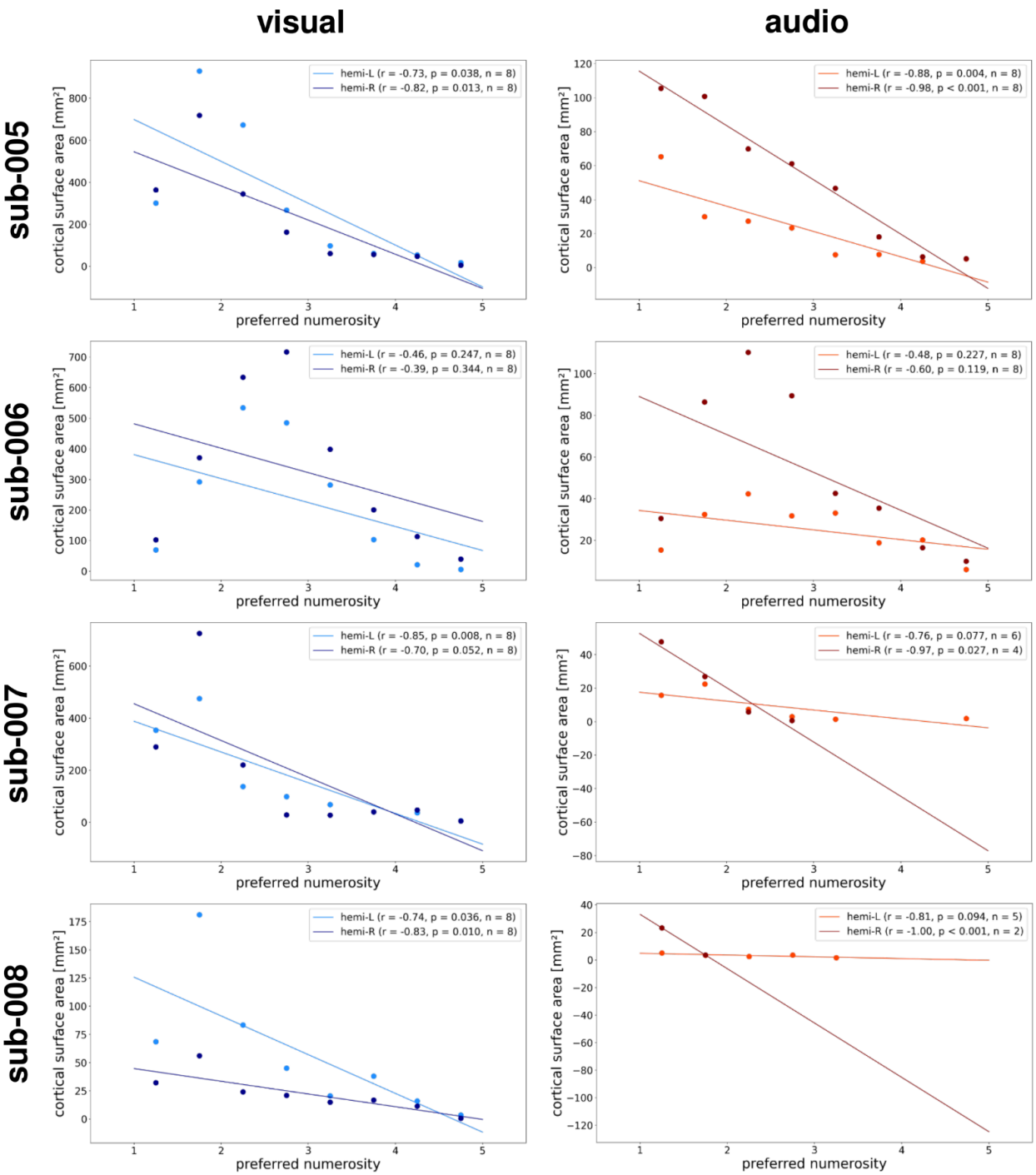

Figure S5: Linear associations between preferred numerosity and surface area (page 2 of 3).

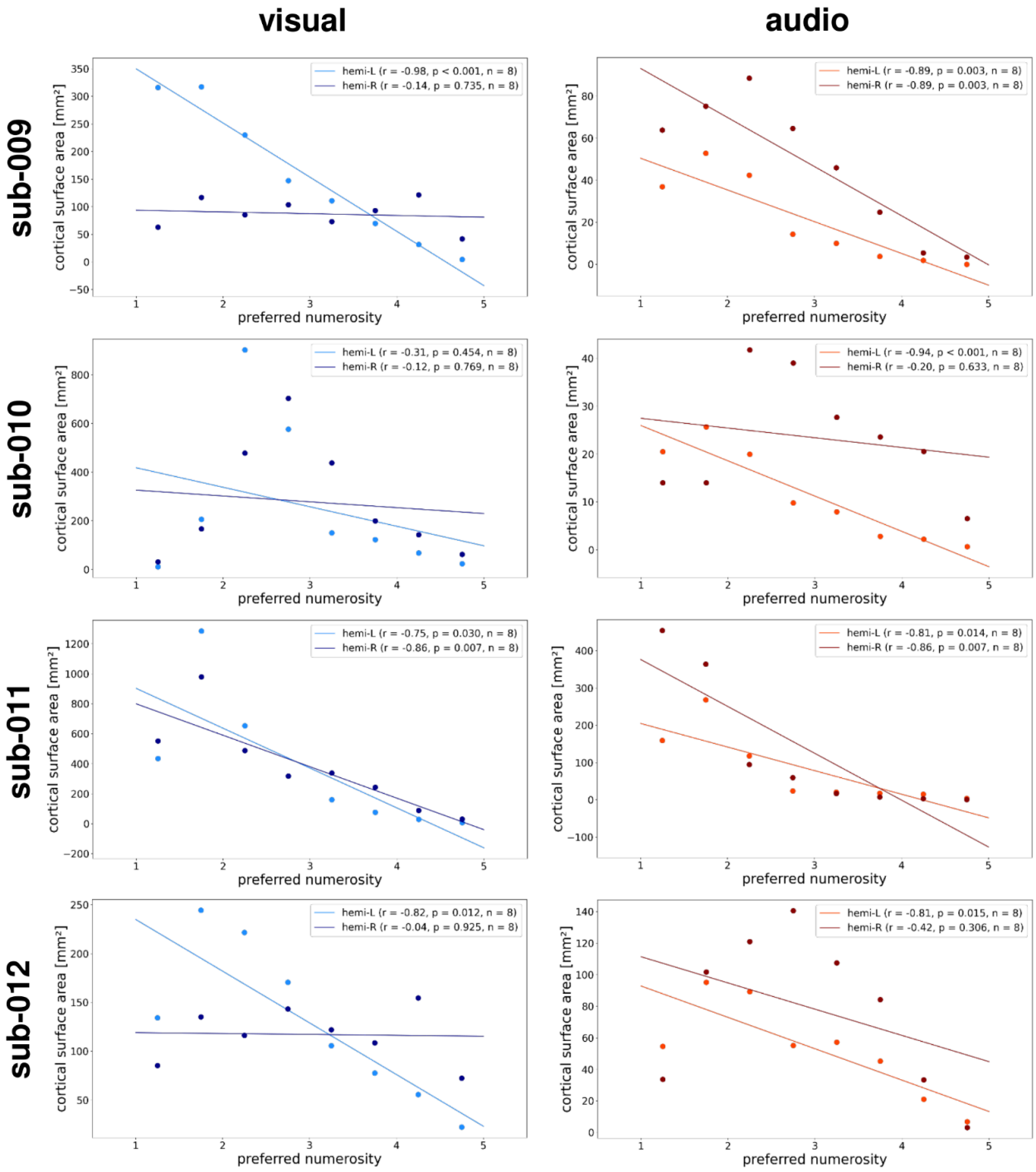

Figure S5: Linear associations between preferred numerosity and surface area (page 3 of 3).

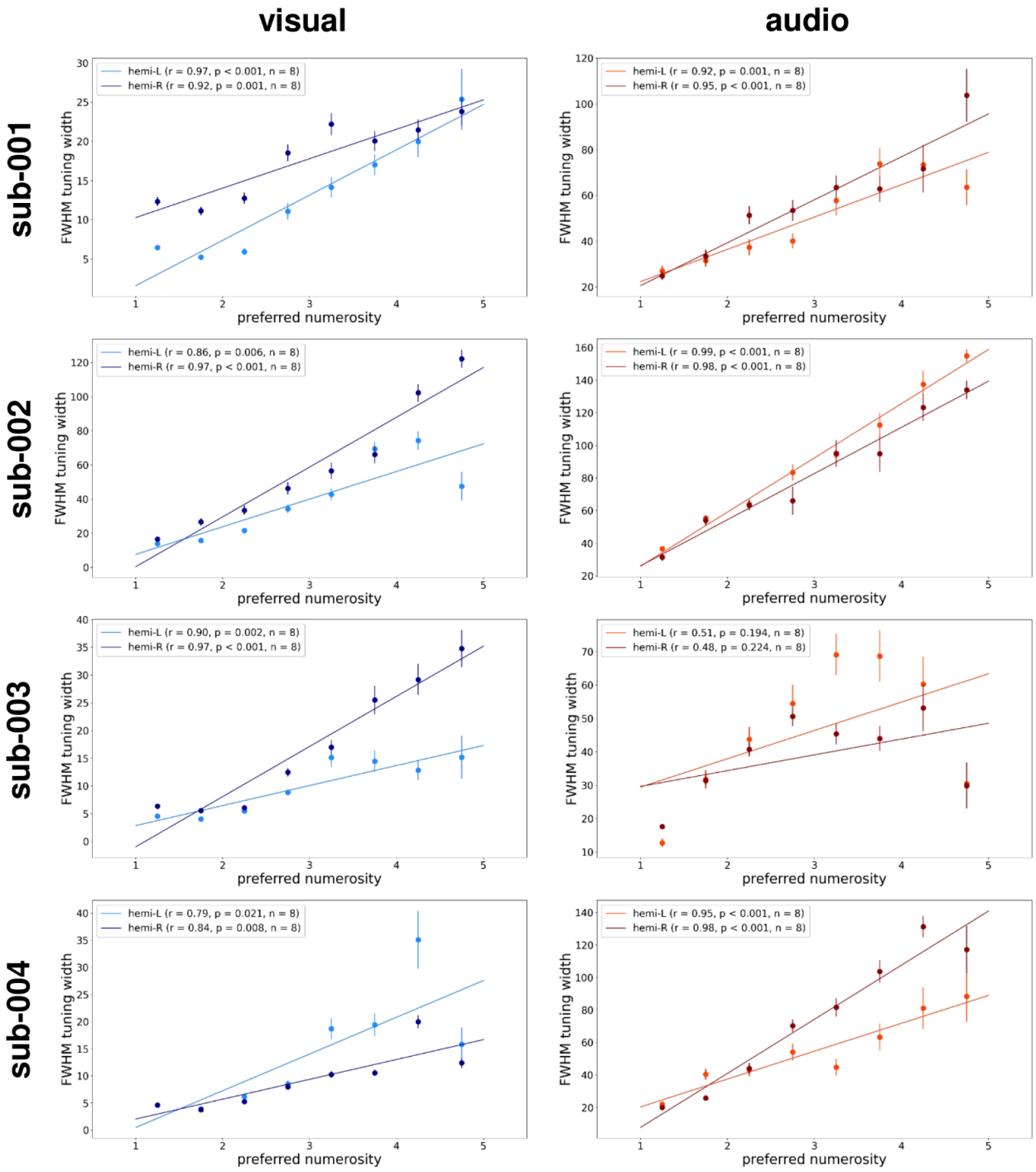

Figure S6: Linear associations between preferred numerosity and tuning width (page 1 of 3). Full width at half maximum (FWHM) increases as a function of preferred numerosity in each subject perceiving either visual (left) or auditory (right) numerosity.

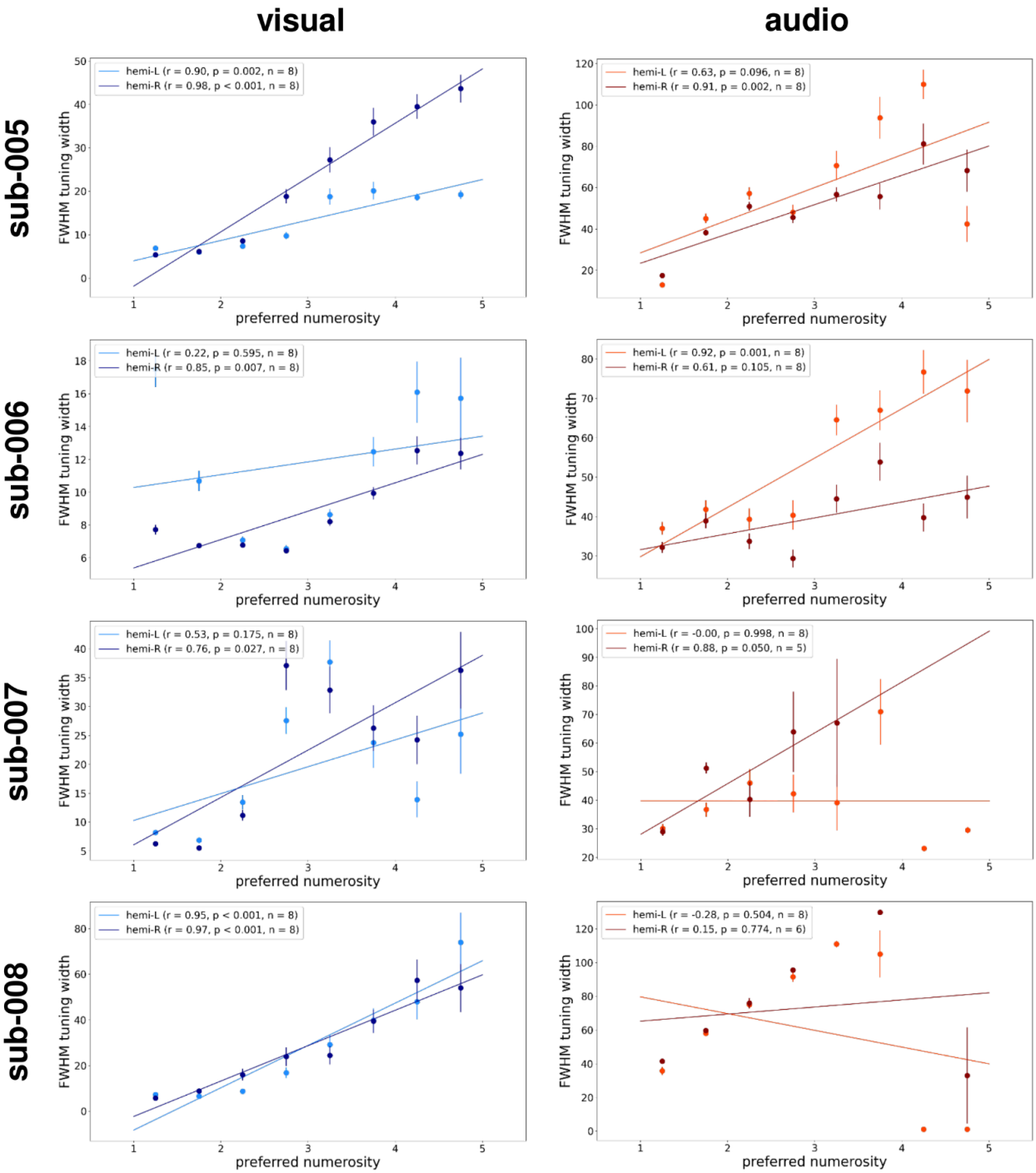

Figure S6: Linear associations between preferred numerosity and tuning width (page 2 of 3).

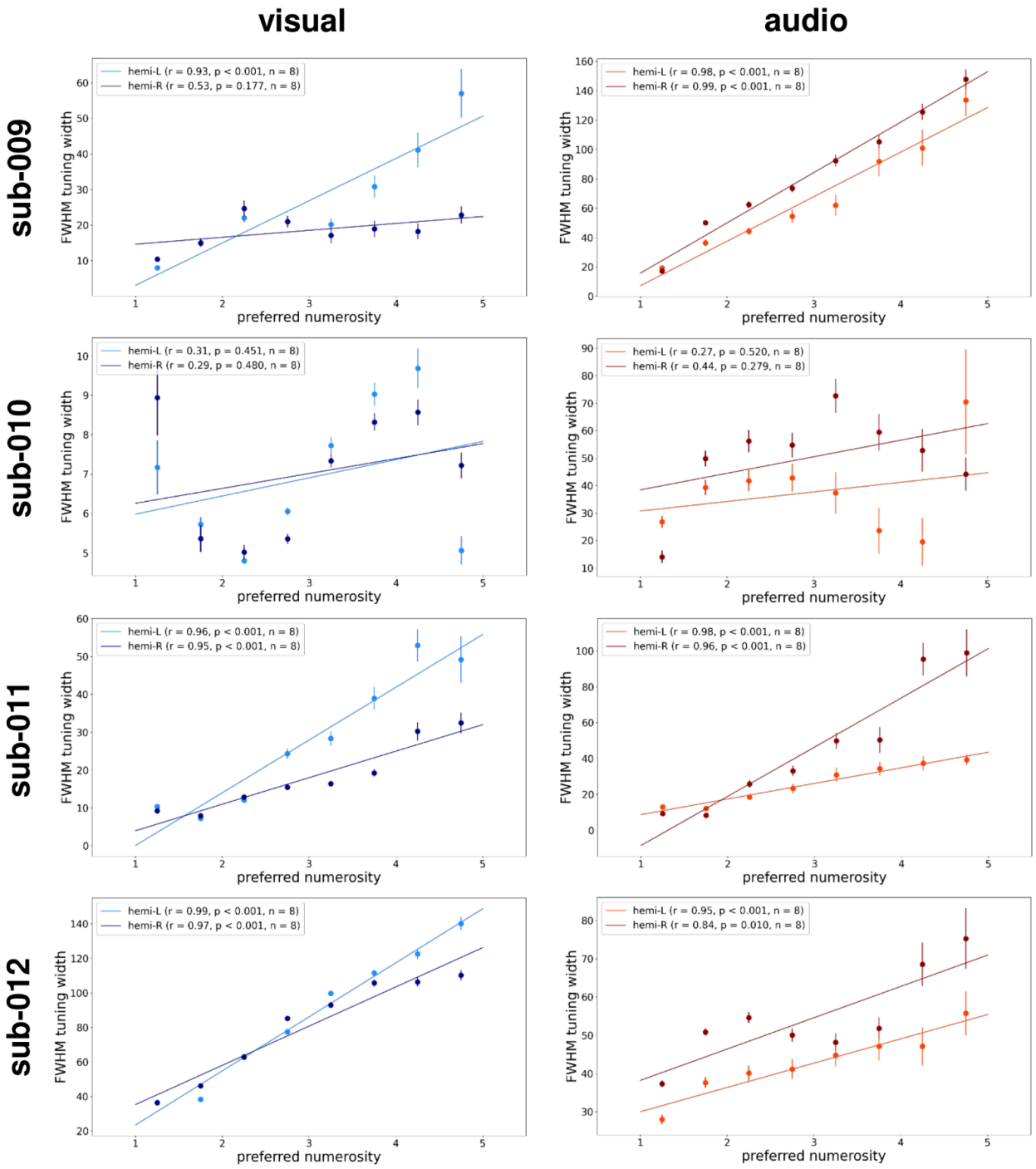

Figure S6: Linear associations between preferred numerosity and tuning width (page 3 of 3).

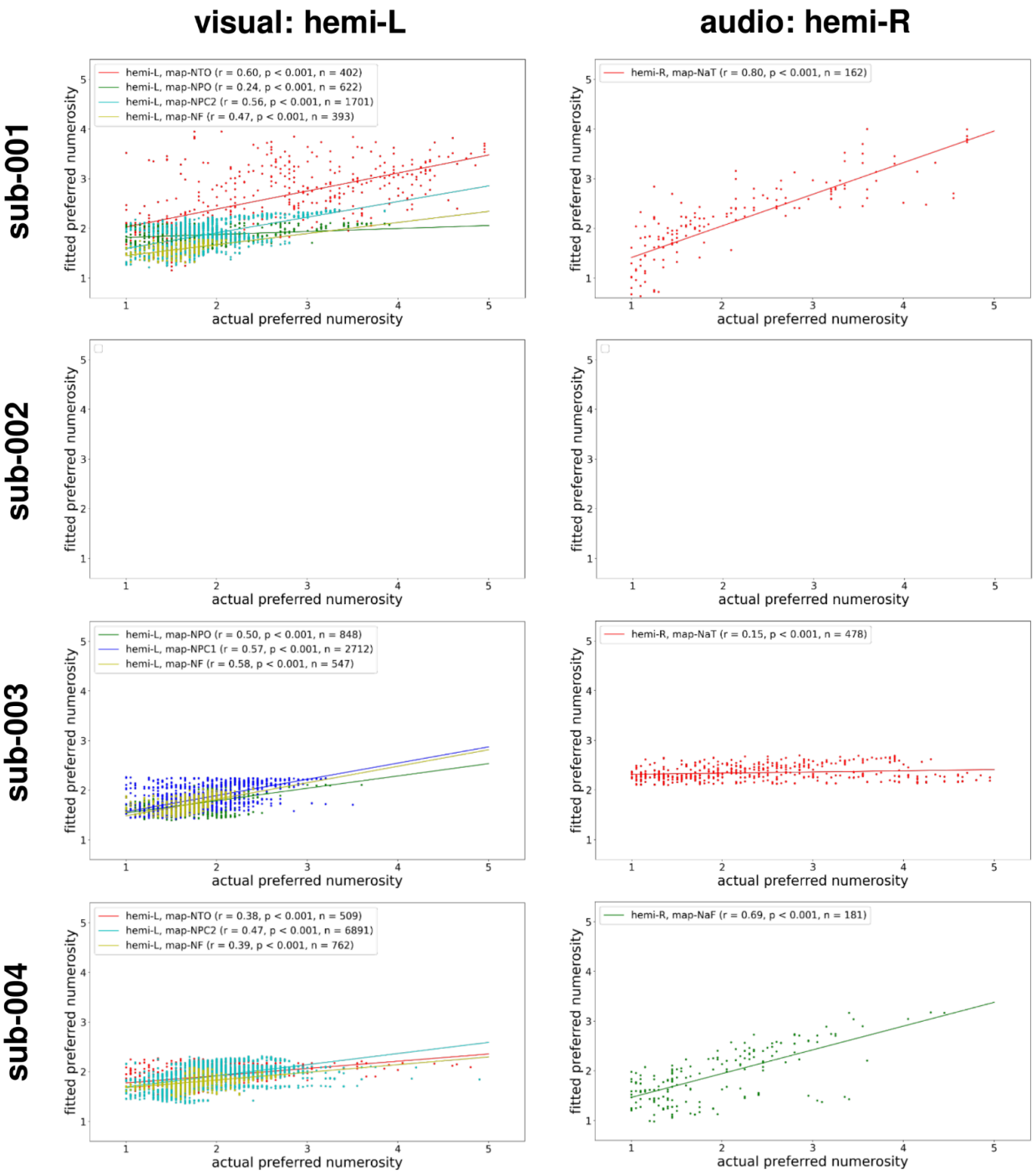

Figure S7: Fitted and preferred numerosity of numerotopic maps (page 1 of 3). Preferred numerosity can be predicted from surface coordinates, indicating a progression of preferred numerosity on the cortical surface within visual and auditory numerotopic maps.

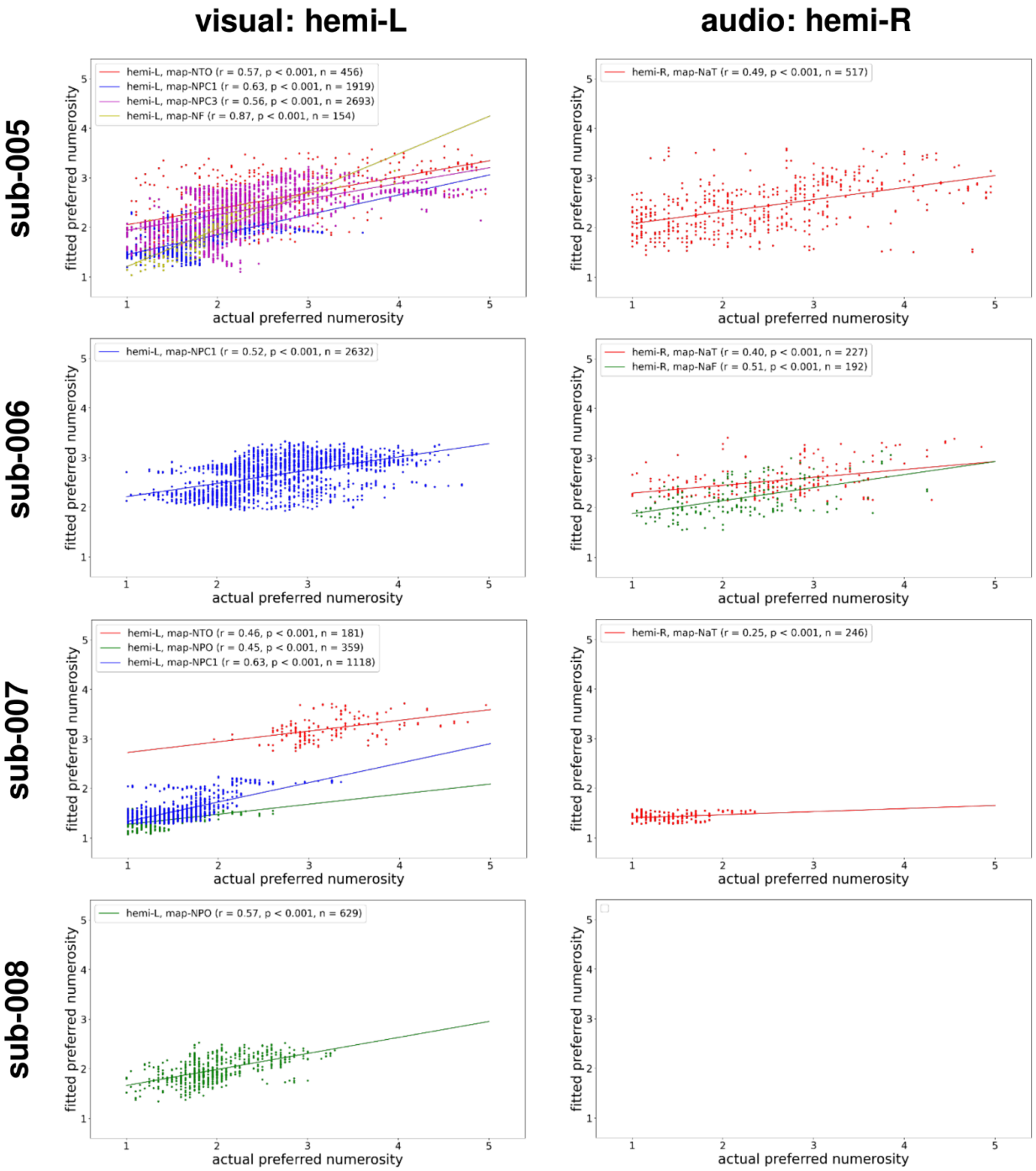

Figure S7: Fitted and preferred numerosity of numerotopic maps (page 2 of 3).

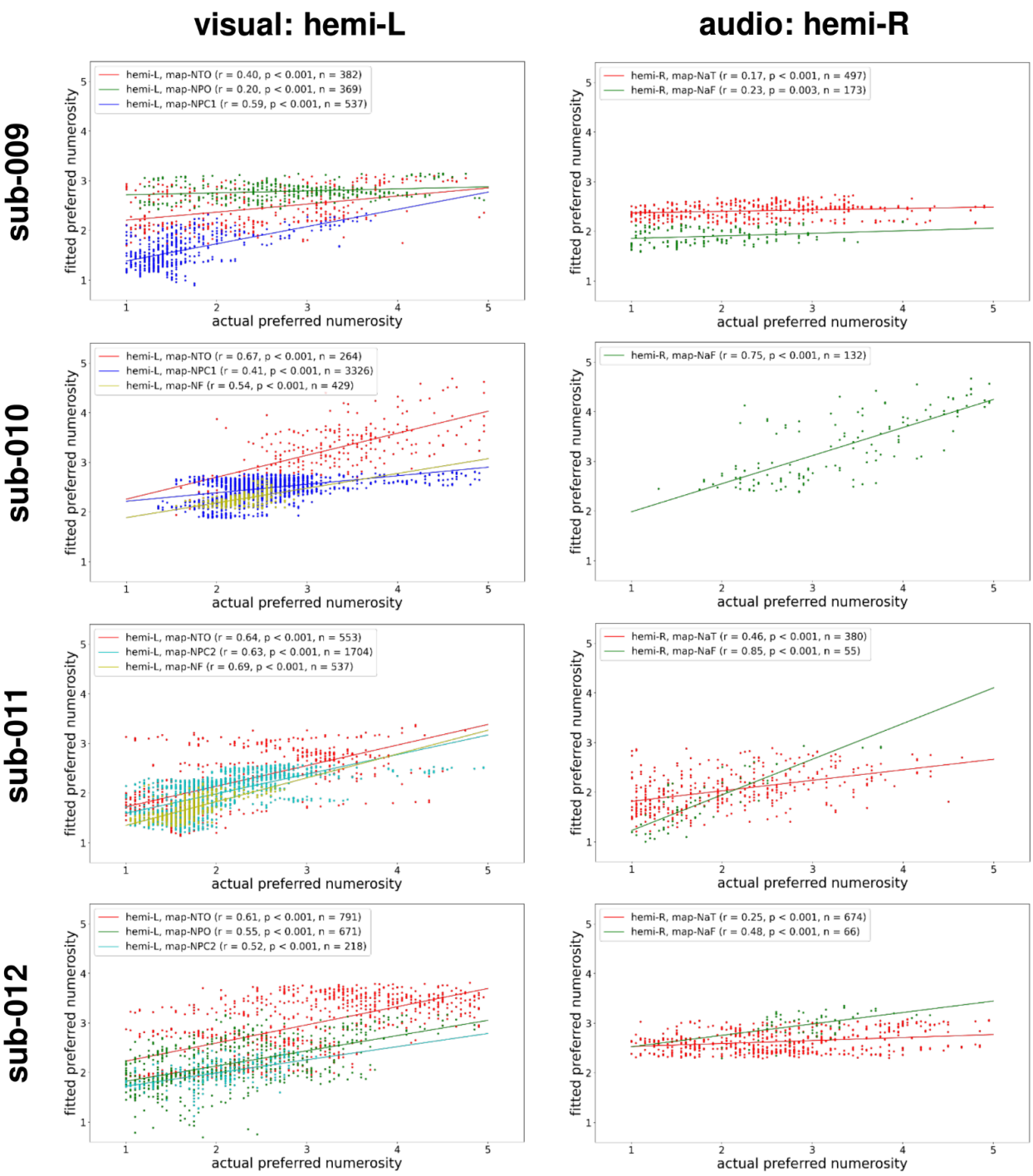

Figure S7: Fitted and preferred numerosity of numerotopic maps (page 3 of 3).

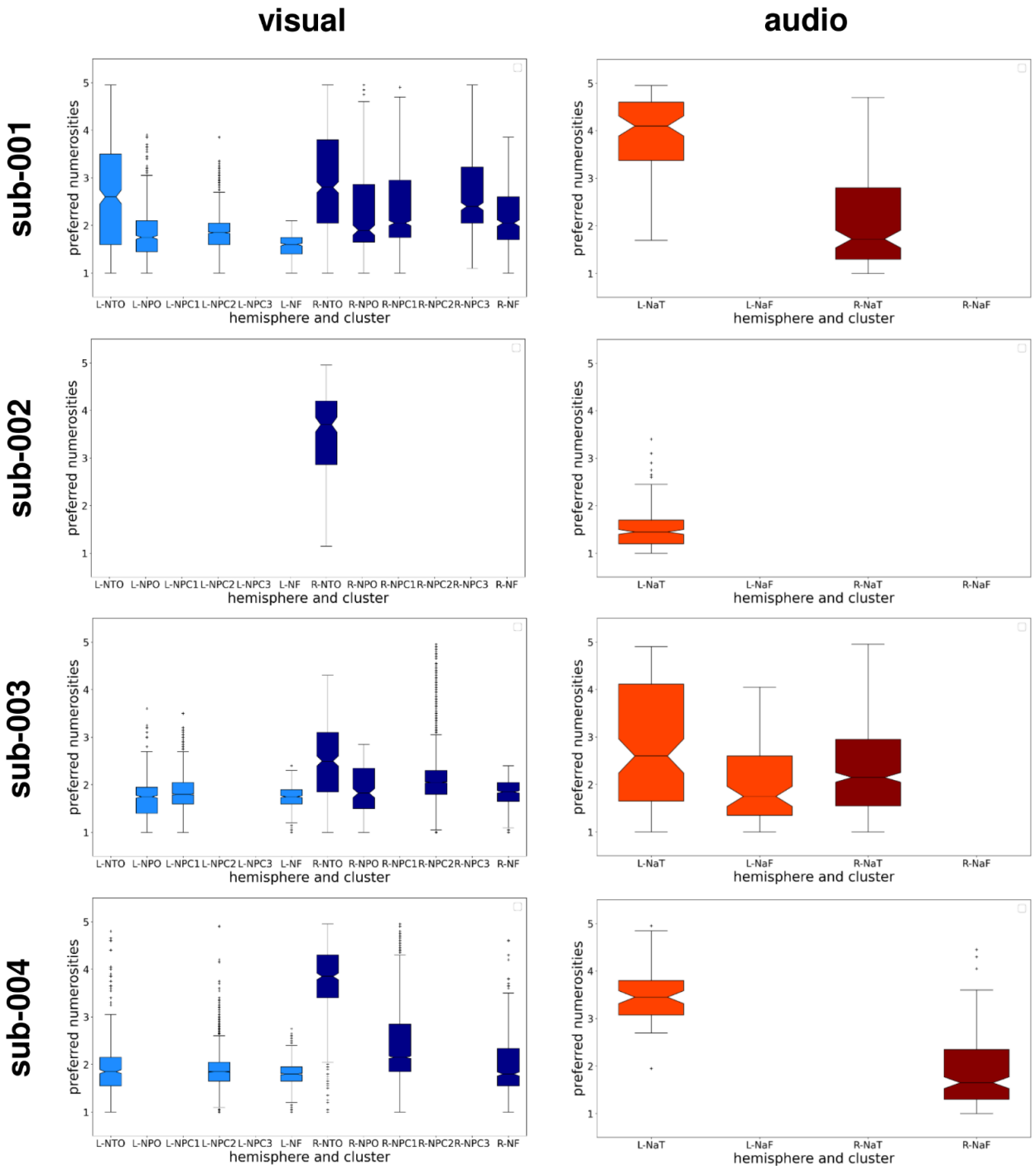

Figure S8: Range of preferred numerosities within numerotopic maps (page 1 of 3). Preferred numerosities of all supra-threshold vertices within up to six visual and up to two auditory numerosity maps per hemisphere are shown as boxplots.

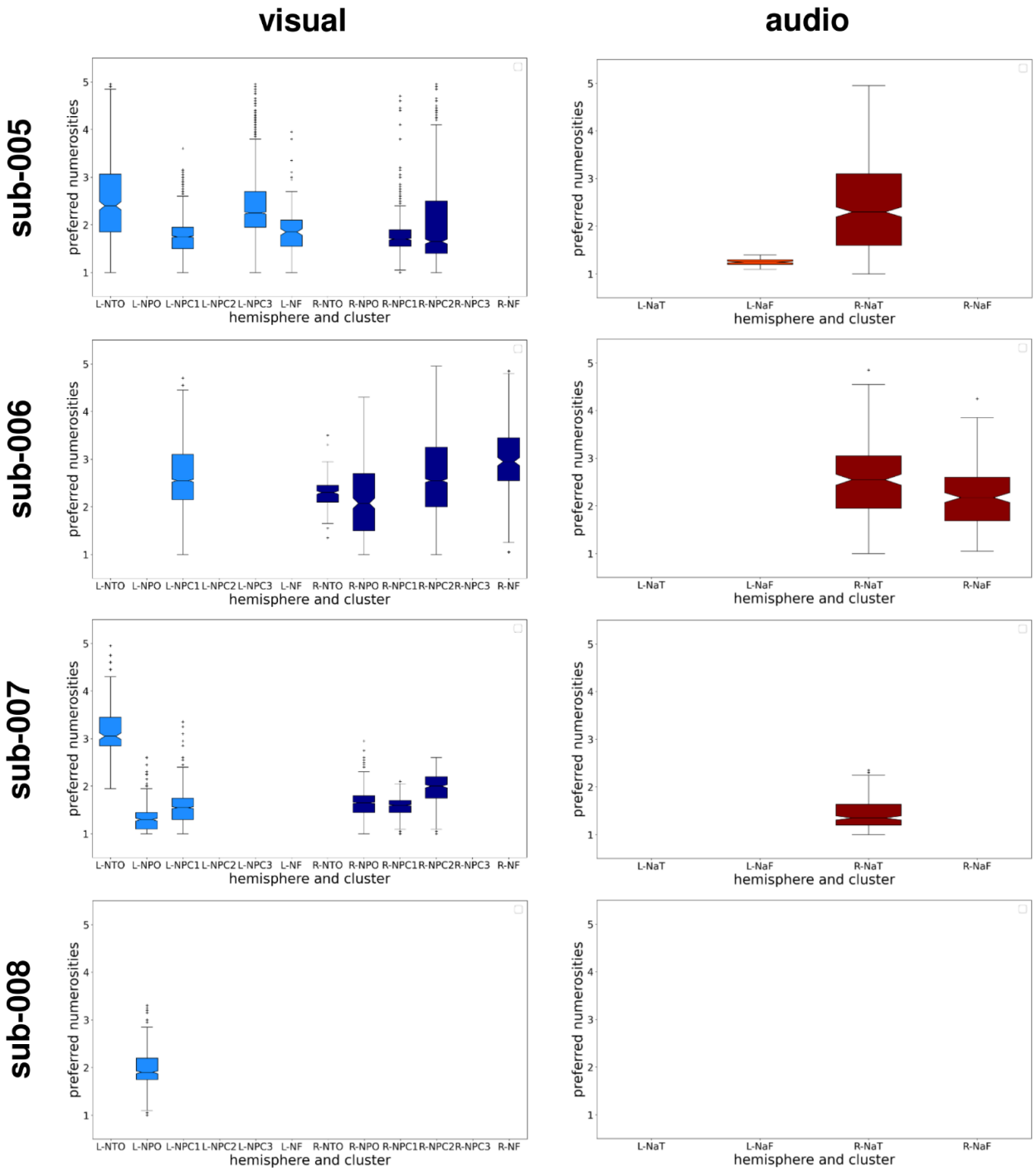

Figure S8: Range of preferred numerosities within numerotopic maps (page 2 of 3).

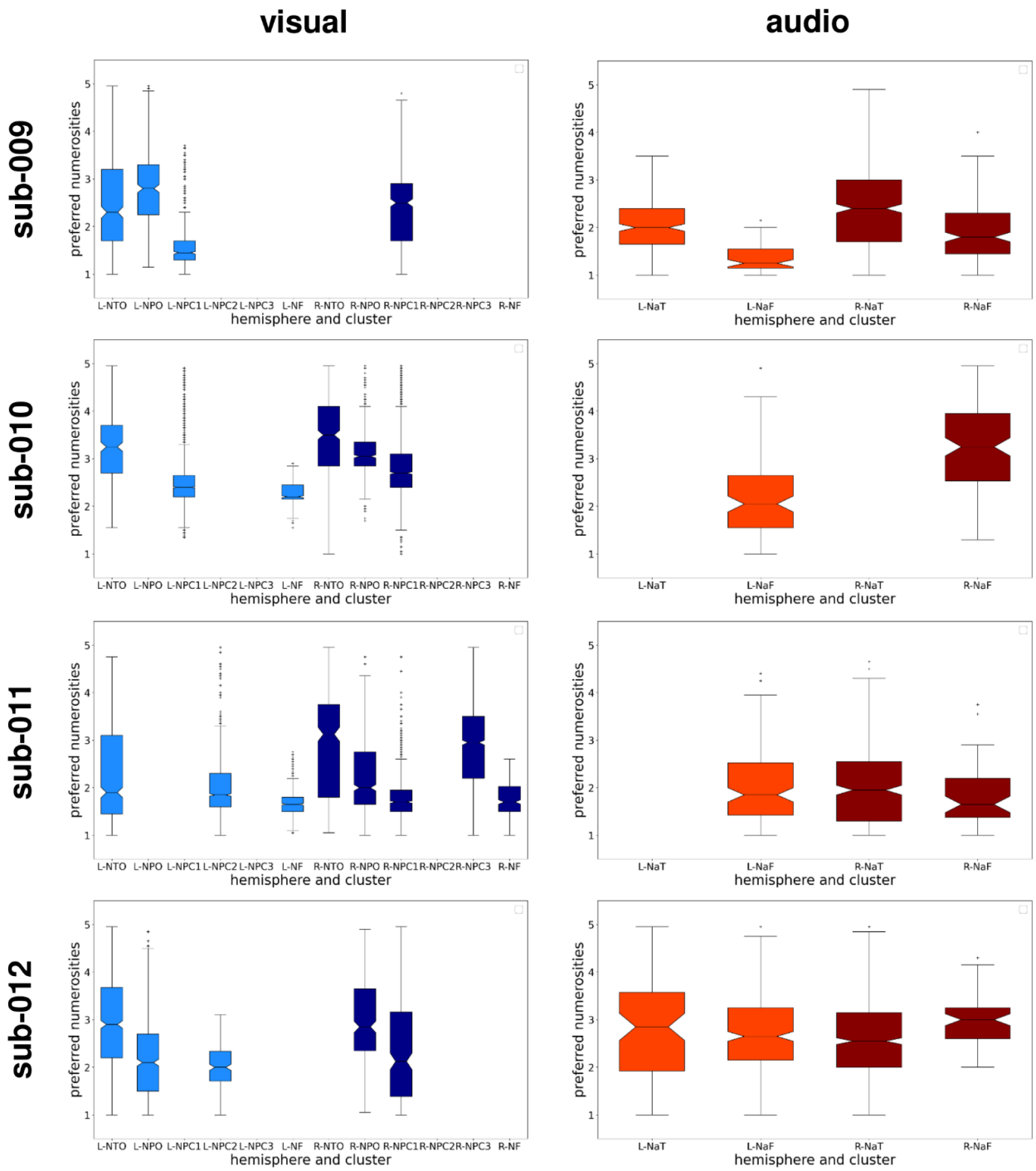

Figure S8: Range of preferred numerosities within numerotopic maps (page 3 of 3).